

PERFORMANCE AND LOADS CORRELATION OF THE UH-60 ROTOR AT HIGH ADVANCE RATIOS

Graham Bowen-Davies

grahambd@umd.edu

Graduate Research Assistant

Inderjit Chopra

chopra@umd.edu

Alfred Gessow Professor and Director

Alfred Gessow Rotorcraft Center

Department of Aerospace Engineering

University of Maryland, College Park, MD 20742

The comprehensive analysis code UMARC is validated at high advance ratios with the UH-60A full-scale slowed rotor test data in a wind tunnel and then used to analyze the high advance ratio aerodynamic environment. UMARC predicts the sensitivity of thrust to collective well up to $\mu = 0.7$, but thrust reversal is predicted at lower collectives (negative) than are evident in the wind tunnel tests. Including a drag model for the blade shank is shown to improve the prediction of rotor drag and the effect of fuselage upwash is shown to further improve the correlation. The sectional normal force shows very good correlation in phase and magnitude and the effect of wake model resolution on the loads is evaluated. Flapwise bending moments at 50% span are well predicted by the analysis up to $\mu = 0.9$. The mean values of the torsional moments are predicted satisfactorily, but the analysis does not capture the high harmonic content.

Nomenclature

AoA	Angle of attack
C_D	Rotor drag coefficient
C_{Droot}	Drag coefficient of blade shank
C_N	Normal force coefficient
C_M	Pitching moment coefficient
C_T	Thrust coefficient
M	Mach number
r	Dimensional radial station
R	Rotor radius
RPM	Revolutions per minute
α_s	Shaft tilt (positive aft)
γ	Lock No.
μ	Advance ratio
σ	Rotor solidity
θ_0	Collective
θ_{1s}	Longitudinal cyclic
θ_{1c}	Lateral cyclic

1. INTRODUCTION

The objective of this paper is to provide new insight into the high advance ratio flow environment by evaluating test data with state-of-the-art, in-house, predic-

tive capability. At high advance ratios, defined here as $\mu > 0.5$, the aeromechanics of the rotor has not been completely comprehended at this time. In order to design the next generation of high-speed rotorcraft, predictive capabilities must be validated against high quality experimental data so that the high advance ratio design space can be understood.

Traditionally, helicopter maximum airspeed has been limited to less than 170 knots (μ of 0.4) by compressibility, dynamic stall and reverse flow aerodynamics causing high power requirements and excessive vibrations. Future vertical lift requirements call for VTOL aircraft that are capable of cruise speeds in excess of 230 knots, a combat range of 400 km, 6K/95° high/hot hover capability and improved efficiency. These combined requirements cannot be met by existing helicopter technology; therefore, the industry is looking at alternative configurations including coaxial rotors, lift offset rotors, tilt-rotors and compound rotors often in combination with rotor rotational speed variation (reduction). As well as the technological challenges faced in achieving efficient rotor speed variation, there is historically a lack of understanding of the flow environment at high advance ratios and limited validation of predictive capability. Developing and validating the current predictive capability requires high quality experimental data.

Until recently, there had been four experiments that

achieved high advance ratios. The Pitcairn PCA-2 Autogiro^[1] was tested in the NACA (predecessor of NASA) full scale wind tunnel in auto-rotation, reaching an advance ratio of 0.7. A 15 ft diameter teetering rotor was tested in the Langley full-scale tunnel up to an advance ratio of 1.45^[2]. A H-34^[3] articulated rotor and a UH-1D^[4] teetering rotor were also tested to high advance ratios in the NASA 40 by 80 foot wind tunnel. Performance data and blade motions from these experiments have been used to evaluate analyses by several researchers^{[5]-[7]}, however these experiments lacked detailed information about the rotor characteristics and the test data were limited in both quality and extent as needed for the validation of modern, higher-fidelity codes.

Recently, the full-scale UH-60A rotor was tested at the U. S. National Full-Scale Aerodynamics Complex (NFAC)^[8]. The slowed rotor portion of this test was conducted to provide a comprehensive set of data from which to learn about high advance ratio aeromechanics as well as providing an opportunity to validate existing modeling capability. Datta, Yeo and Norman^[9] provided a comprehensive evaluation of the results as well as a fundamental explanation of the reverse flow physics. There have been several papers dealing with correlation of comprehensive analyses to the UH-60A full-scale data. Kottapalli^[10] and Yeo^[11] have both applied CAMRAD II^[12] to the high advance ratio results and have shown generally good prediction of performance and loads, although correlation degraded as advance ratios approached 1.0. Ormiston^[13] used RCAS to offer additional insights to the performance correlation and directed focus on the control reversal phenomenon as a function of retreating blade stall. Potsdam, Datta and Jayaraman^[14] used a coupled Helios/RCAS CFD-CSD analysis that showed good correlation of the sectional forces and offered insight into the aerodynamic behavior and wake interactions of the slowed rotor. In particular, the visualization of the aerodynamics and wake formation at the blade root was shown to be important. Authors^[16] showed preliminary correlation of performance and sectional airloads using UMARC, and investigated the role of wake modeling resolution in the sectional load prediction.

At the University of Maryland, Berry and Chopra^{[17]-[20]} have carried out Mach-scaled rotor (of UH-60A) tests on twisted and untwisted 4-bladed articulated rotors in the Glenn L. Martin wind tunnel. The most recent test extended the advance ratio boundary up to $\mu = 1.4$ and measured rotor performance, blade root motion and structural loads as well as obtained some limited pressure data. These tests provided a unique comparison of model-scale data to the full scale UH-60A tests to investigate the role played by blade twist as well as scaling effects. Authors^[21] investigated these results with UMARC

showing good correlation of performance including advance ratios beyond thrust reversal. It was further shown that UMARC could satisfactorily predict vibratory loads up to $\mu = 1.4$. Berry and Chopra^[22] have recently repeated the wind tunnel tests up to $\mu = 1.4$ to generate a complete data set using distributed pressure sensors.

The UH-60A data is the focus of this paper. The objective of the current work is to evaluate the predictive capability of the comprehensive rotorcraft analysis UMARC to predict the performance and loads at high advance ratios. The analysis is then used to study aspects of high advance ratio aeromechanics. A brief description of the wind tunnel test and the test conditions will be followed by a description of UMARC. The results will first correlate performance, sectional airloads and bending moments.

Table 1. UH-60A blade properties.

100% RPM	258
Radius (ft)	26.833
Solidity	0.0826
Lock No. (γ)	7.0
Airfoil	SC1095
	SC1094r8
Twist	-16°
Sweep	20° at 93%

Table 2. Test conditions for the UH-60A tests.

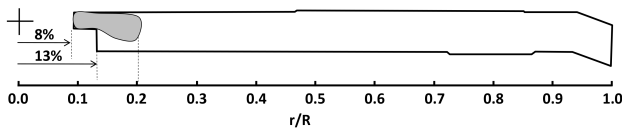
RPM Variation	40%
Shaft Angle (Degrees)	0°, 4° (aft)
Wind Speed (knots)	50-175
Advance Ratio	0.3-1.0

2. DESCRIPTION OF UH-60A WIND TUNNEL TEST

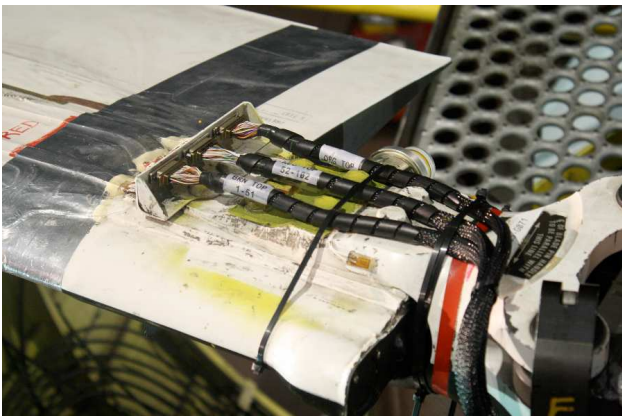
A full-scale UH-60A rotor was tested in the U. S. National Full-Scale Aerodynamics Complex (NFAC) 40 by 80 ft wind tunnel at NASA Ames. The rotor was mounted on the NFAC Large Rotor Test Apparatus (LRTA) as shown in Fig. 1a. A part of the testing included slowing the rotor with an objective of achieving high advance ratio edgewise flight in order to explore the aeromechanics of this unconventional flight regime. The rotor was set to 100%, 65% and 40% of nominal operating rotational speed (258 RPM) to achieve tip Mach number of 0.65, 0.42 and 0.26 respectively. The rotor shaft angle was set to 0°, 2° and 4° (aft). For each test condition, the collective was set and the cyclics were used to trim the rotor to zero first harmonic flapping at the blade root.



(a) Full-scale UH-60A rotor installed on the Large Rotor Test Apparatus in the NFAC 40- by 80- ft wind tunnel.



(b) UH-60A blade planform.



(c) UH-60A instrumented blade shank.

Fig. 1. UH-60A root geometry

The instrumented rotor blades were the same as those used during the airloads flight tests of the UH-60A Black Hawk^[23] although they were refurbished for the wind tunnel test. Instrumentation pertinent to this paper included pressure transducers placed between 22.5% and 99% spanwise stations; although, during the slowed rotor testing phase, only the 22.5%, 86.5% and 92% maintained enough working transducers to gather sectional airloads data. Strain gauges were placed between 13.5% and 90% stations to gather blade bending information. Instrumentation at the blade root measured flap, lag and pitch motions. The shaft, hub, pitch links and LRTA stand were instrumented to measure rotating and fixed frame steady and vibratory loads. For a full description of the experimental setup see the description by Datta et al.^[9].

Important properties of the rotor are listed in Table 1. Figure 1b shows the planform of the UH-60A blade and a detail of the blade shank for the instrumented blades is shown in Fig. 1c. The aerodynamics of the root section requires careful treatment, particularly at high advance ratios. The aerodynamics of the root cut-out (typically modeled at 20%) are normally assumed unimportant at advance ratios for typical rotorcraft. Yeo^[11], Ormiston^[13] and Potsdam et al.^[15] suggested that the drag of the rotating shank is important for a good prediction of rotor axial (drag) loads and total power. Potsdam et al. used CFD to model this region and suggested that an approximate shank drag (c_d) of 0.14-0.18 is appropriate while Yeo used $c_d=0.4$ to get good correlation of rotor total drag force. Potsdam et al. further showed that the region between 13% and 20% provides 50%-80% of the lift of the adjacent clean blade.

A summary comparing the test conditions is given in Table 2

3. UMARC MODELING

The University of Maryland Advanced Rotor Code (UMARC)^[24] was used as a baseline platform for this study. The blades are modeled as second order, nonlinear, isotropic, Euler-Bernoulli beams capable of 15 degrees of freedom and allow for coupled flap, lag, torsion, and axial motion. The equations of motion are solved using a variational methodology with modal reduction in conjunction with finite elements in space and time. 20 spatial elements and 12 time elements were used in this study, while 10 coupled blade modes are used in modal analysis. The lifting-line aerodynamic model implements quasi-steady aerodynamics by means of a table look-up for section lift, drag, and pitching moment coefficients. Near wake is modeled via a Weissinger-L representation and assumed to trail 30° behind the rotor in-plane with the trailing edge. The trailed wake is discretized into three azimuthal segments and the radial discretization is chosen to align with the aerodynamic discretization so as to minimize interpolation errors. The far-wake is modeled by the Bagai-Leishman relaxation free-wake model^[25]. Convergence studies were conducted by evaluating the available sectional airloads data. A 10° azimuthal discretization of the wake with 2 turns of wake tracking gave satisfactory resolution at high advance ratios. The far-wake can be represented by an arbitrary number of wake trailers with increasing computational cost. For these results, at least two wake trailers were necessary to capture the sectional airloads. One trailer is defined to release from the blade tip with a circulation strength nominally equal to the peak blade circulation. A second is released only when there is a change in sign of circulation along the blade, typically arising on the advancing side of

twisted rotors. The second trailer, called the inboard trailer in these results, is assumed to be shed at the point where the circulation changes sign along the blade radius and the circulation at the tip trailer is adjusted appropriately. In addition to the dual wake trailer model, a prescribed root trailer released from the inboard blade extent proved to have some influence on the aft rotor loads and was included in the analysis. Unsteady airloads that model attached and separated flow, and dynamic stall are captured by the Leishman-Beddoes unsteady model^[26] but is not included in reverse flow region.

The wind tunnel test used fixed collective and zero first harmonic flapping at the blade root as the trim target and this approach was followed in the analysis. The nominal shaft angles are corrected to account for tunnel wall corrections. The coupled blade response and the root flapping constraints are solved iteratively to obtain the blade deflections and trim control settings.

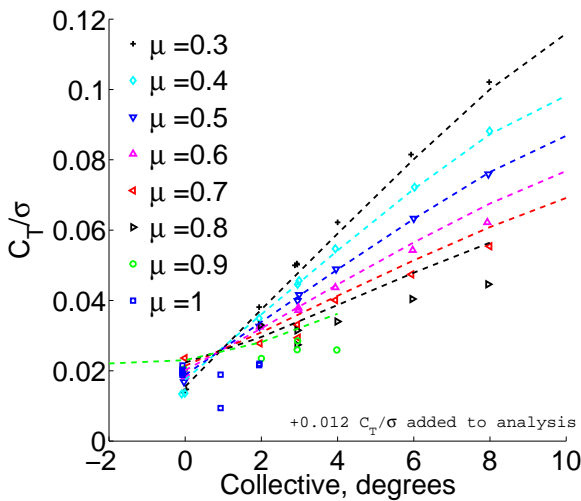


Fig. 2. Thrust vs. collective for increasing advance ratios, $M_{tip} = 0.26$, 0° shaft angle. (Symbols: Test, - - Analysis)

4. RESULTS

4.1 Rotor Performance

The prediction of thrust (C_T/σ) against collective setting for advance ratios increasing from $\mu = 0.3$ - 0.9 is shown in Fig. 2. The predictions from the analysis are uniformly incremented by $\Delta C_T/\sigma = 0.012$ (about 440 lb) to counter an unexplained thrust offset at 0° collective. The sensitivity of thrust to collective is well predicted at all collectives up to $\mu = 0.6$. At $\mu = 0.7$, the data shows more scatter but the analysis consistently over-predicts the thrust (with the thrust off-set correction). For $\mu = 0.8$ and 0.9 , neither the slope nor the

thrust magnitude are well predicted for positive collectives, and trim results for $\mu = 1.0$ could not be calculated. The prediction of thrust near thrust reversal (the advance ratio beyond which thrust decreases with increasing collective) gets complicated because of limited understanding of the reverse flow aerodynamics. Investigating negative collectives at $\mu = 0.9$ shows that the sensitivity of thrust to collective is nearly flat before a change in slope near 0° collective. The analysis predicts thrust reversal occurring at lower collectives than shown in the test. Authors^[21] showed similar results with a Mach scaled rotor model, showing that the onset of thrust reversal was defined by the onset of reverse flow stall. Prediction of the conditions when the airfoil stalls in reverse flow is sensitive to root cut-out, blade twist, shaft angle and airfoil stall characteristics in reverse flow. The root cut-out and the blade pre-twist are both well characterized for the UH-60A rotor; while, elastic twist variation is difficult to evaluate experimentally and the highly unsteady nature of reverse flow stall needs further experimental investigation to improve current models. Unsteady airloads in the reverse flow are discussed further in the discussion on sectional airloads correlation.

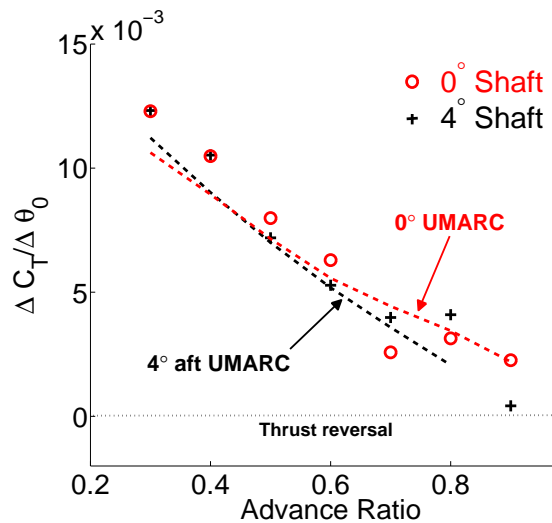


Fig. 3. Δ Thrust vs. Δ collective for increasing advance ratios, $M_{tip} = 0.26$. (Symbols: Test, - - Analysis)

Thrust results are also available for the 4° aft shaft angle case and the correlation with analysis is similar to the 0° cases. Figure 3 compares the slope of the thrust vs. collective results at each advance ratio for the two shaft angles (the slope is evaluated for small positive collectives). For the 0° shaft tilt case, the slope of the analysis veers away from linear above $\mu = 0.7$ which corresponds to where the analysis starts to have trouble predicting the onset of reverse flow (note that the slope of the negative collective cases for $\mu = 0.9$ lies on the linear trend). For the 4° aft shaft tilt, the

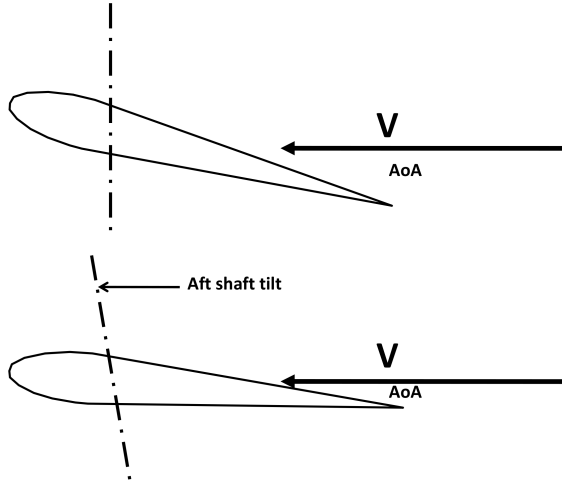
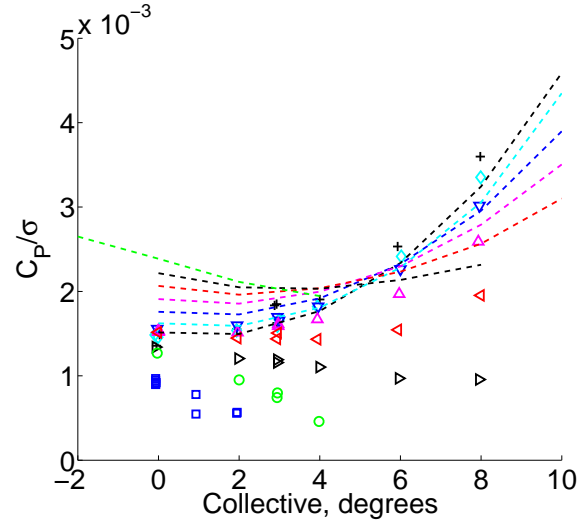


Fig. 4. Schematic showing the impact of aft shaft angle on reverse flow angle of attack for fixed pitch angle.

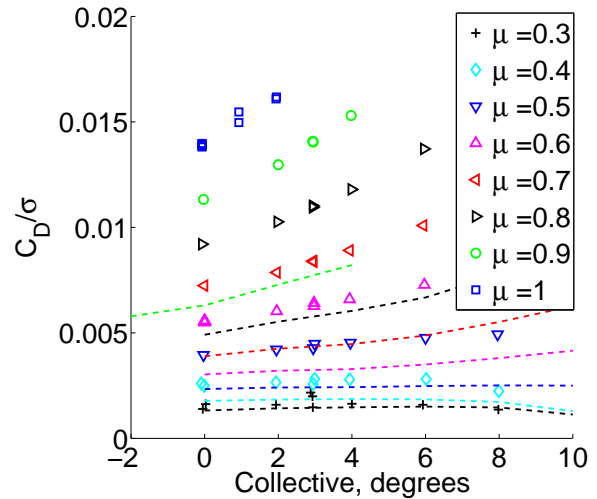
trend remains nearly linear to $\mu = 0.8$ in better agreement with the test. Aft shaft tilt effectively reduces the reverse flow angles of attack (Fig. 4) for a constant collective (and longitudinal cyclic) and delays reverse chord stall to higher collectives.

Figure 5 shows the prediction of shaft power and rotor drag force against collective for increasing advance ratio for a 0° shaft angle. For these cases, the drag associated with the blade shank is not yet modeled. The correlation of shaft power is fair at $\mu = 0.3$, but degrades for an increasing advance ratio. The analysis globally over-predicts shaft power; and, the analysis predicts increasing power with advance ratio at zero collective while power is decreasing with advance ratio in the test data. Validation of the UH-60A rotor model against flight tests up to $\mu = 0.38$ have shown very good prediction of shaft power and the poor correlation seen here is unexpected. The analysis does predict decreasing slope at increasing advance ratios with nearly no change in shaft power with increasing collective at $\mu = 0.8$ in agreement with the experiment.

The rotor drag force is significantly underpredicted without including the shank drag. Without any physical information to base the drag of the shank on, a trial and error approach was used to arrive at a $C_{Droot} = 0.4$ in the region inboard of 20% radial station. The resulting correlation of power and drag with the test is shown in Fig. 6. While the zero collective drag force values now match the test for all advance ratios, the increasing drag force with collective is underpredicted. The additional root drag increases shaft power, degrading correlation further. A second discrepancy between the baseline analysis and the test is the fuselage. The LRTA fuselage shown in Fig. 1a



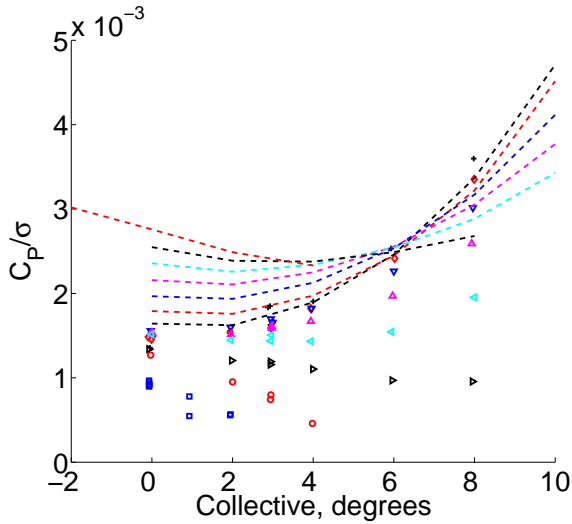
(a) Shaft power vs. collective



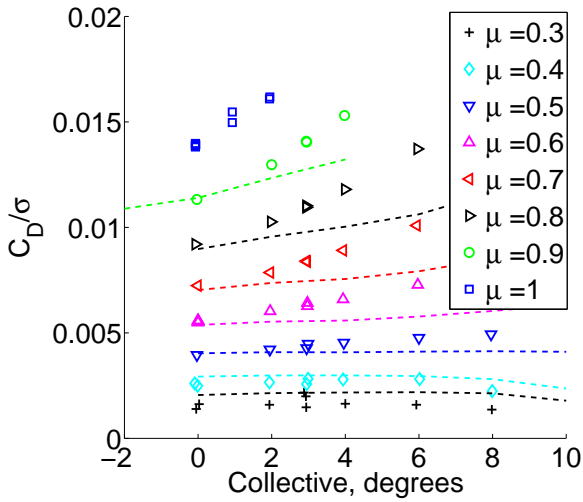
(b) Rotor drag vs. collective

Fig. 5. Shaft power and rotor drag vs. collective for increasing advance ratios, $M_{tip} = 0.26$, 0° shaft angle. (Symbols: Test, - - Analysis)

is expected to induce an upwash at the front of the rotor disc and possibly a downwash on the rear disc. Fuselage upwash effects are not yet modeled carefully in UMARC; however, a primitive account of fuselage upwash can be achieved by altering the inflow locally and the resulting power and rotor drag (including shank drag) are shown in Fig. 7. Although there are no available measurements of this effect from the UH-60A tests, Amiraux et al.^[27] used CFD to simulate the upwash from the HART rotor. This result was used to approximate the impact of the fuselage as a circular region of upwash that scales linearly with advance ratio. The circle of upwash was centered at $r/R = 0.5$ on the front of the rotor, with a non-dimensional radius = 0.25. The upwash was scaled from the results of Amiraux et al. to give $\lambda_{upwash} = 0.2\mu$. Figure 7 shows two effects that support a role played by the



(a) Shaft power vs. collective

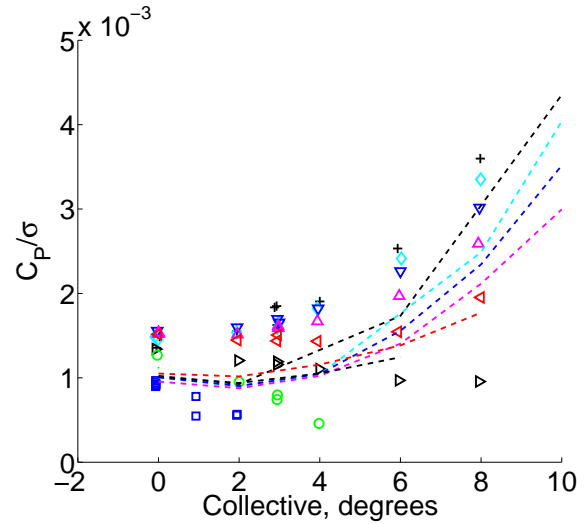


(b) Rotor drag vs. collective

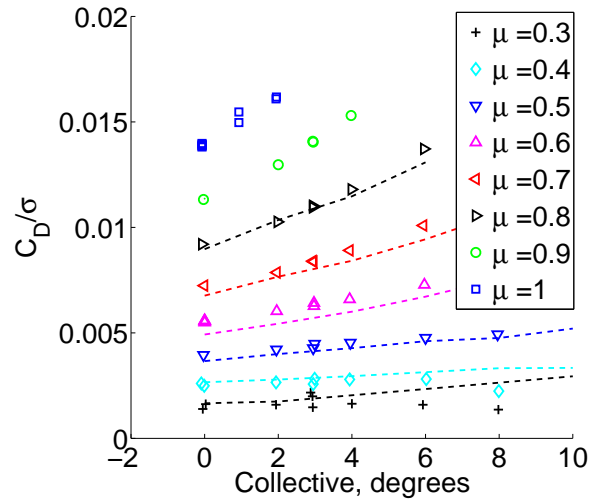
Fig. 6. Shaft power and rotor drag vs. collective for increasing advance ratios, $M_{tip} = 0.26$, 0° shaft angle, $C_{Droot} = 0.4$ (Symbols: Test, - - Analysis)

fuselage in the rotor performance. The power prediction is closer to the experiment while maintaining the correct trends, and the trend of the drag force gives much better agreement with the test results. This result is meant only to show the sensitivity of the analysis to the presence of a fuselage while a more comprehensive fuselage model is required to draw strong conclusions.

The trimmed control cyclics vs. thrust for the advance ratio sweep are shown in Fig. 8 (for $C_{Droot} = 0.0$, but the impact of root drag is small). Overall, the longitudinal cyclic is satisfactorily predicted, but degrades with advance ratio. The trend exhibited at $\mu = 0.9$ repeats what was seen in the thrust behavior and shows a change in trend corresponding to zero collective. The lateral cyclic is overpredicted by the analysis by up to 2° and there is no sign of the reversing



(a) Shaft power vs. collective



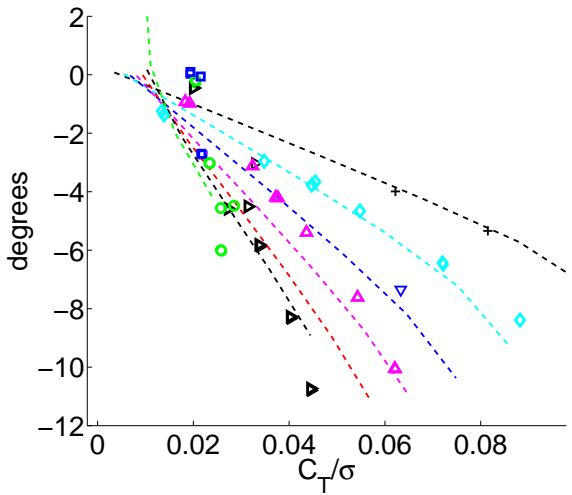
(b) Rotor drag vs. collective

Fig. 7. Shaft power and rotor drag vs. collective for increasing advance ratios, $M_{tip} = 0.26$, 0° shaft angle, $C_{Droot} = 0.4$, including fuselage model (Symbols: Test, - - Analysis)

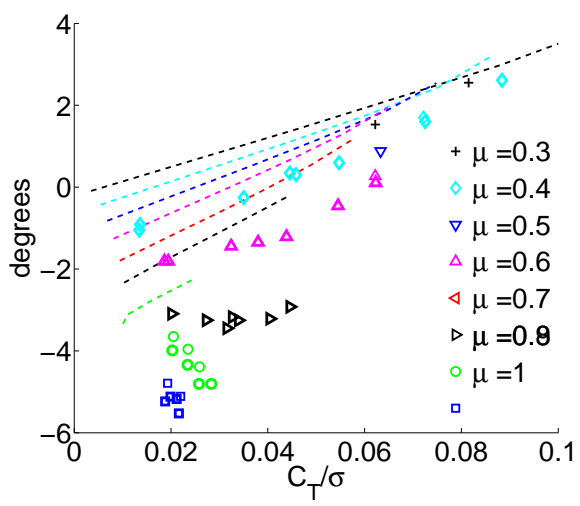
trend at high advance ratio seen in the test data. The predictions of the lateral cyclic by some other comprehensive codes have been quite good and the reasons for discrepancy shown here are unknown.

4.2 Sectional Airloads

The sectional normal force prediction and correlation at $r/R = 92\%$ for a 0° shaft angle is shown in Fig. 9 for advance ratios of 0.3, 0.5 and 0.6. The rotor thrust was trimmed to $C_T/\sigma = 0.062$ (approximately) in the wind tunnel test for each of the cases. The analysis is trimmed to the corresponding collective, which gives a good overall correlation of the sectional loads despite generally under predicting thrust. The aerody-



(a) Longitudinal cyclic vs. thrust

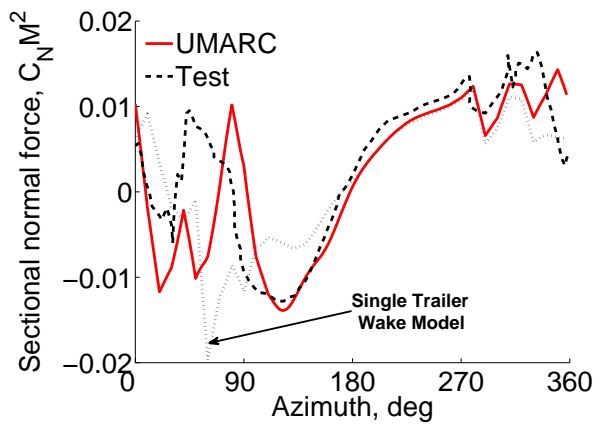


(b) Lateral cyclic vs. thrust

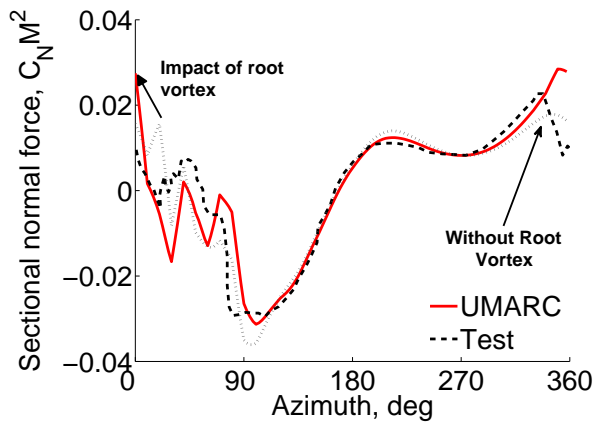
Fig. 8. Trim cyclics collective vs. thrust for increasing advance ratios, $M_{tip} = 0.26$, 0° shaft angle, $C_{Droot} = 0.4$ (Symbols: Test, - - Analysis)

dynamic model includes dual wake trailers from the outboard rotor as well as a prescribed wake trailer from the blade root.

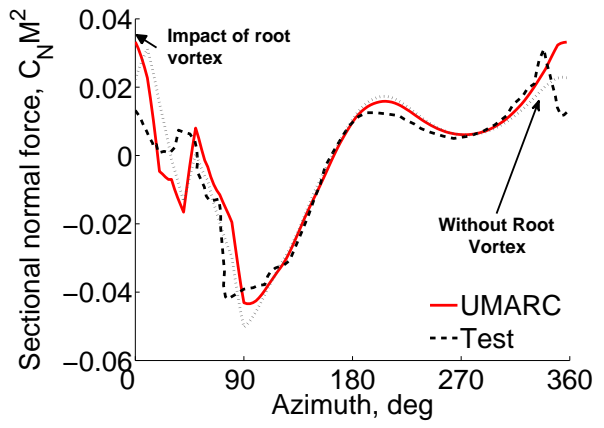
The normal force correlation is quite good and all the key features of the loads are captured for each advance ratio. The magnitude and phase of the negative lift on the advancing rotor (near 90°) is well predicted. Both the test and analysis show the point of peak negative loading moving aft with increasing advance ratio. The loading on the front of the rotor shows a smooth variation of normal force as this is relatively clean aerodynamic environment (the wake is quickly washed downstream). At an advance ratio of 0.3, near an azimuth of 330° , a blade vortex interaction (BVI) between the blade and the wake trailer from the previous blade is represented well by the analysis. At higher advance ratios, the wake is swept



(a) $\mu = 0.3$



(b) $\mu = 0.5$

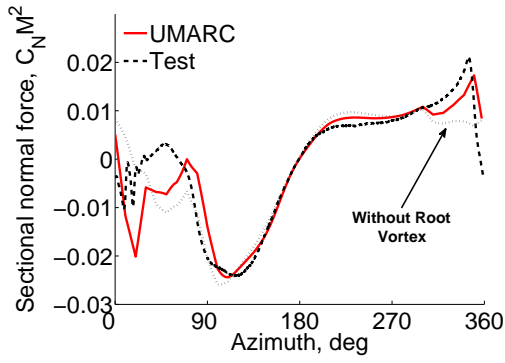


(c) $\mu = 0.6$

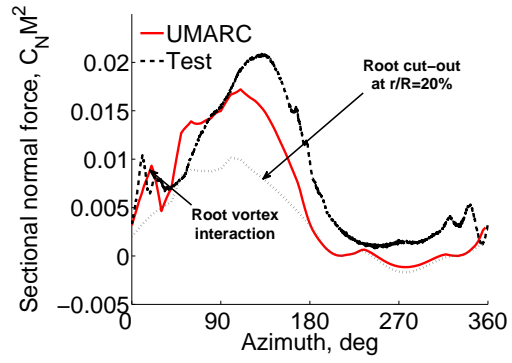
Fig. 9. Sectional normal force ($C_N M^2$), $r/R = 92\%$, $C_T/\sigma = 0.062$, $\alpha_s = 0^\circ$.

above and behind the rotor before successive blades can interact with it. On the aft rotor, between 330° and 90° azimuth, both the wind tunnel data and the analysis show higher frequency content, but a one to one correlation is less clear. In each case, the analysis appears to over-predict the magnitude of the oscillations.

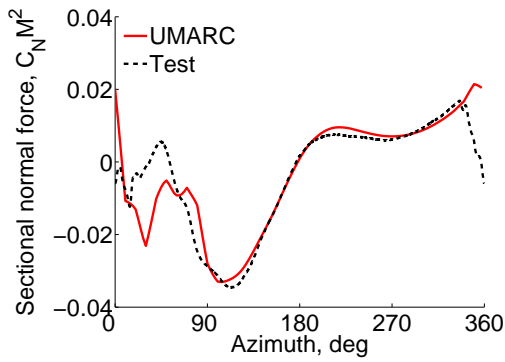
In order to better understand the important aspects



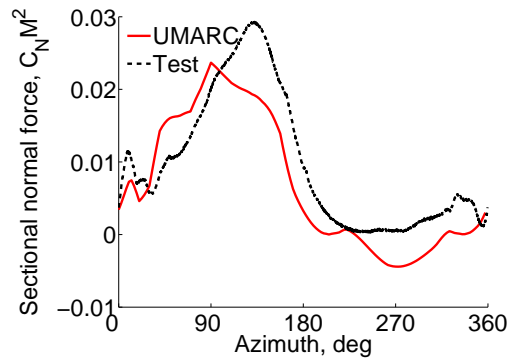
(a) $\mu = 0.4$



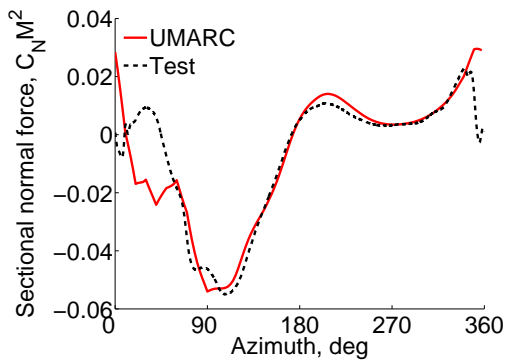
(a) $\mu = 0.4$



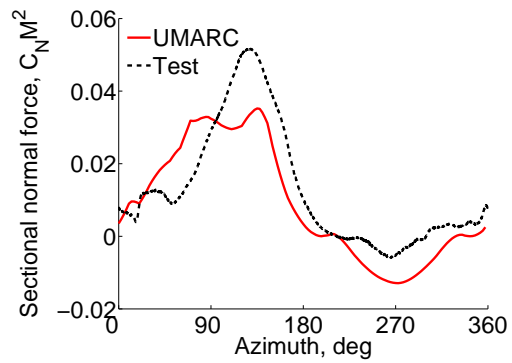
(b) $\mu = 0.5$



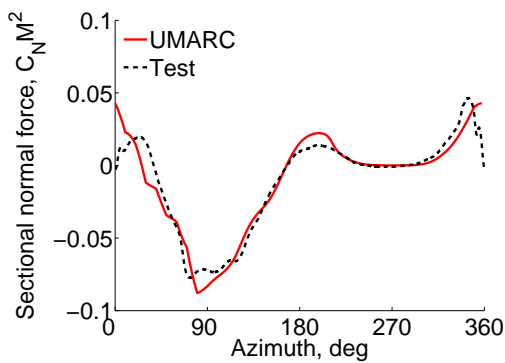
(b) $\mu = 0.5$



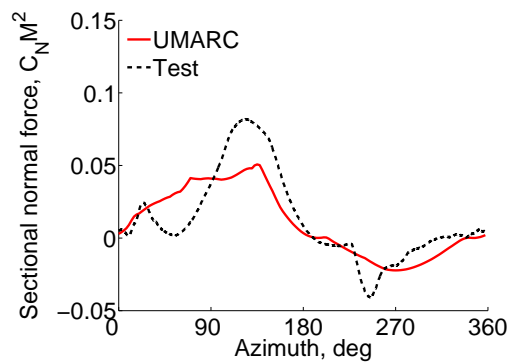
(c) $\mu = 0.7$



(c) $\mu = 0.7$



(d) $\mu = 0.9$



(d) $\mu = 0.9$

Fig. 10. Sectional normal force ($C_N M^2$), $r/R = 92\%$. $C_T/\sigma = 0.062$, $\alpha_s = 4^\circ$ aft.

Fig. 11. Sectional normal force ($C_N M^2$), $r/R = 22.5\%$. $C_T/\sigma = 0.062$, $\alpha_s = 4^\circ$ aft.

of the aerodynamic model for the normal force correlation, included in the figures are results with simplified analyses. Figure 9a includes a dotted line which represents the normal force when a single wake trailer (no root trailer either) is modeled. The front of the rotor is not affected and the BVI at 330° azimuth remains well represented. The advancing side shows a larger impact of the wake modeling. Without the second trailer, the negative loading near 90° azimuth is underpredicted and there is a strong blade vortex interaction at 60° azimuth which contributes towards a large over-prediction of the negative lift in the first quadrant.

The experimental data shows a lift drop off at $\approx 335^\circ$ that remains consistent with advance ratio. The analysis predicts a similar behavior, although this occurs at a later azimuth (between 350° and 10° azimuth). Figure 9b includes the normal force prediction for the dual wake model but excluding the root vortex as the dotted line. Comparing the result on the aft rotor with and without the root trailer shows that the root trailer impacts the impulsive loading. The root trailer appears to entrain the inboard tip trailer from the leading rotor blade. This process impacts where the rotor blade interacts with the inboard trailer and this determines most of the aft loading, rather than interaction of the root trailer directly. This is highlighted in Fig. 9b which shows that the peak near 30° azimuth (dotted line) is pulled ahead in azimuth by the presence of the root trailer. Two wake modeling assumptions are likely to impact this interaction. Firstly, the current model assumes that the root vortex follows a helical, prescribed trajectory. Secondly, the inboard wake trailer is assumed to release from the point of zero circulation along the blade. A more rigorous modeling of both trailers may improve the normal force prediction on the aft rotor.

The sectional normal force prediction for 0° shaft angle, at 92% radial station, shows good agreement when matching collectives despite the analysis underpredicting total thrust. The differences are in the first quadrant are small as are the absolute magnitude of the forces. Sectional loads at inboard stations are not yet available for the 0° shaft tilt cases, but are available for the 4° aft shaft tilt cases where the thrust is similarly underpredicted by the analysis. 22.5%, 89% and 92% radial stations are available for advance ratios between $\mu = 0.4-0.9$. The 92% station is shown in Fig. 10 for these advance ratios and shows similar, good, correlation for 4° aft as for 0° shaft angle cases. The $\mu = 0.4$ case, shown in Fig. 10a, does a particularly good job at capturing the root vortex interaction near 330° but is generally predicted at later azimuth for higher advance ratios. Not shown, but the 86% radial location shows qualitatively similar correlation.

At the 22.5% station, the experimental results show that the advancing side (second quadrant) is

generating a significant lifting force. Comparison of the normal force to the 92% radial station shows that a significant portion of the total lift is generated at inboard stations. The typical UH-60A model that has been validated in UMARC at normal advance ratios ($\mu < 0.4$) assumes a 20% root cut-out which does not contribute lift (nor drag generally) to the rotor forces. The $\mu = 0.4$ case includes a dotted line that represents the predicted results of these assumptions. The analysis significantly under-predicts the advancing side lift. The CFD results of Potsdam et al.^[15] suggest that the inboard region (13%-20%) produces lift and that there can be a root trailer from near 13% radial station. The implication of this for the 22.5% radial station is that less down-wash is felt from the rolled up wake at the root since this now occurs further inboard. The correlation of advancing side lift is significantly improved with the inclusion of the inboard aerodynamic stations; although, the magnitude remains somewhat underpredicted and continues to contribute to the under-prediction of rotor thrust.

The retreating side is not affected by the inboard vortex modeling. Up to $\mu = 0.7$, the analysis overpredicts the negative lift on the retreating blade where the test shows the normal force to be benign. The magnitude of the predicted reversed lift is small and does not significantly contribute to the thrust underprediction (this can be demonstrated by setting the reverse flow negative lift to zero with minimal change in thrust). The $\mu = 0.9$ case is shown in Fig. 11d and shows a large impulsive lift in the reverse flow region. This appears to be reverse chord dynamic stall which provides a lift increment. The analysis does not model dynamic stall in reverse flow and cannot capture this, which is important for predicting thrust reversal. The presence of the dynamic stall vortex maintains a strong negative lift in reverse flow that gives a net reduction in thrust. Without the vortex, the reverse flow airfoil stalls, reducing negative lift and halts thrust reversal at a lower collective than with the dynamic stall vortex. This helps to explain the change in thrust behavior seen for $\mu = 0.9$ in Fig. 2.

Finally, the test shows a spike in normal force at early azimuths for all advance ratios. This is an interaction with a trailed root vortex and is well predicted by the analysis.

Figures 12 and 13 show the sectional pitching moments for $\mu=0.4 - 0.9$ for the 4° aft shaft angle at 22.5% and 92% span locations respectively. There is a mean offset in the pitching moment data between the experiment and analysis (reported by Potsdam et al. and which remains unexplained), which has been removed to aide comparison. At the 22.5% station (the y-axis scale has been equalized) the correlation is generally poor and the pitching moment is highly overpredicted by the analysis in the reverse flow re-

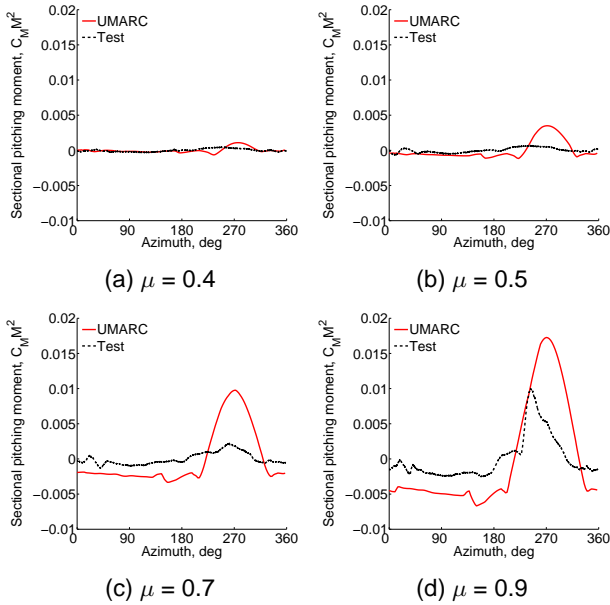


Fig. 12. Sectional pitching moment ($C_M M^2$), $r/R = 22.5\%$. $C_T/\sigma = 0.062$, $\alpha_s = 4^\circ$ aft.

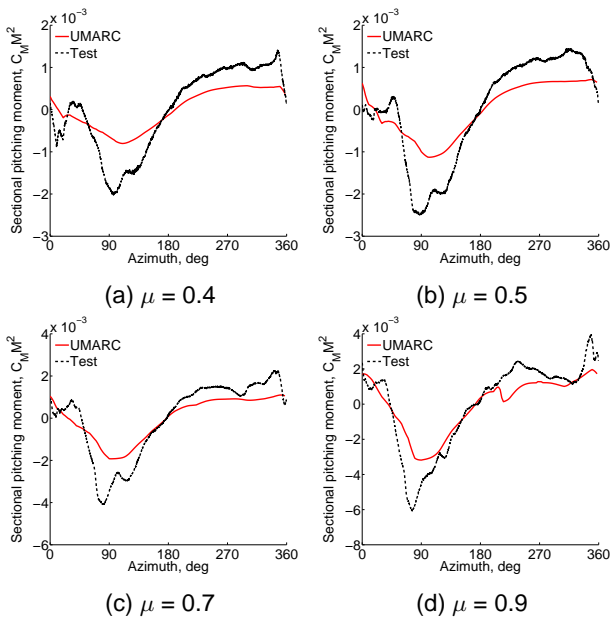


Fig. 13. Sectional pitching moment ($C_M M^2$), $r/R = 92\%$. $C_T/\sigma = 0.062$, $\alpha_s = 4^\circ$ aft.

gion. It has been suggested that part of the discrepancy arises from insufficient pressure taps to accurately resolve pitching moment. A second source of error is from the available pitching moment tables that do not account for Mach number or Reynolds number effects in reverse flow. At $\mu = 0.9$, the test shows evidence of reverse flow dynamic stall supporting the result shown in the normal force. The trend of the pitching moment at 92% span is represented by the analysis, but the peak advancing side moment and details are not well resolved. The aerodynamic envi-

ronment is benign and better pitching moment predictions are expected.

Table 3. Blade frequency variation at 100% and 40% RPM

	100% (/rev)		40% (/rev)	
1 st Mode	0.276	(L)	0.317	(L)
2 nd Mode	1.037	(F)	1.048	(F)
3 rd Mode	2.83	(F)	3.39	(F)
4 th Mode	4.44	(T)	10.94	(T)
5 th Mode	4.68	(F/L)	7.64	(F)
6 th Mode	5.18	(F)	11.27	(F)

4.3 Structural Loads

The first 6 blade frequencies for the UH-60A rotor are listed in Table 3 for the baseline (100% RPM) and the slowed rotor (40% RPM). The first torsion frequency changes significantly from 4.44/rev to near 11/rev and the 5th Flap/Lag coupled mode increases to 7.6/rev leaving only the second flap in the region of 4/rev with its frequency at 3.39/rev.

Figure 14 shows the oscillatory (1/rev and up) flap bending moments at 50% span for the 4° aft shaft tilt cases. The predicted oscillatory loads show very good agreement with test data in the second, third and fourth quadrants although peak bending moment in the second quadrant is somewhat underpredicted with a small phase error. The first quadrant prediction reflects the challenges seen in the normal force prediction of the highly unsteady loading. The vibratory harmonics (3, 4 and 5/rev) of flap bending, shown in Fig. 15, show a strong 3/rev content from the second flap mode. The analysis has a small phase error, but the magnitude and trends appear correct for the $\mu = 0.4$ and 0.5 cases with a small degradation in magnitude correlation at $\mu = 0.7$ and 0.9. The phase remains well represented for all advance ratios. The modal analysis may contribute partially to the phase error because the blade modes are found about the blade at the collective setting and cannot account for cyclic variations to blade pitch.

The oscillatory torsional moments are shown in Fig. 16 and the vibratory harmonics are shown in Fig. 17 for the 4° aft shaft angle cases. The mean trend of oscillatory torsional moments at 50% span location are quite well predicted by the analysis but the measured data contains higher harmonics (>12/rev) than are captured by the analysis. The analysis predicts some 11/rev blade torsional response owing to the placement of the 1st torsion mode near 11/rev. Figure 16a includes a single case that was run using 20 time elements and 30 blade modes (blue dotted line) to ensure that the missing higher harmonics in

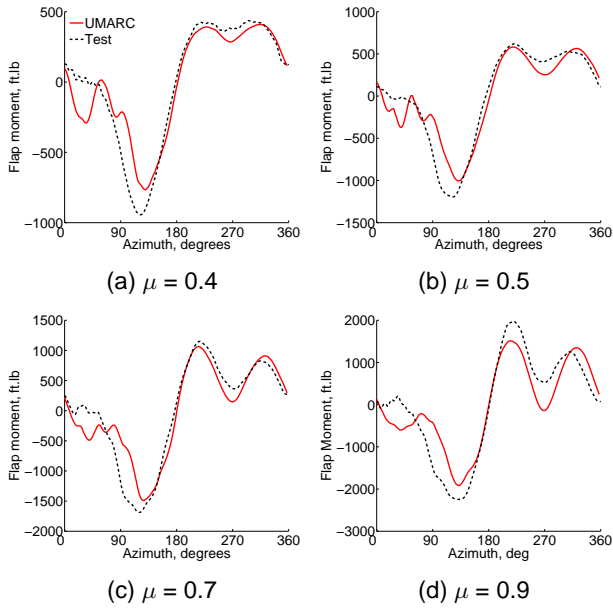


Fig. 14. Oscillatory flap bending moment, $r/R = 50\%$. $C_T/\sigma = 0.062$, $\alpha_s = 4^\circ$ aft.

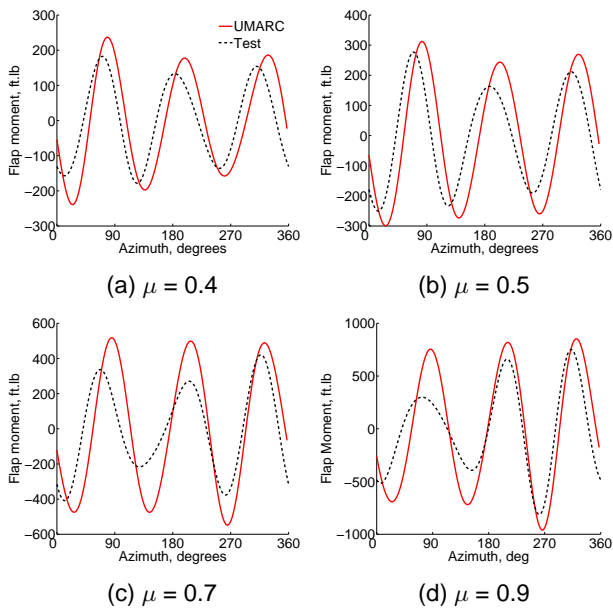


Fig. 15. Vibratory (3-5/rev) flap bending moment, $r/R = 50\%$. $C_T/\sigma = 0.062$, $\alpha_s = 4^\circ$ aft.

the analysis were not due to insufficient modeling degrees of freedom. The differences between the two analyses remain small. The vibratory harmonics are well predicted at $\mu = 0.4$ and 0.5 but break down at $\mu = 0.7$. At $\mu = 0.9$, the dynamic stall on the retreating side appears to excite a large torsional response that is not predicted by the analysis.

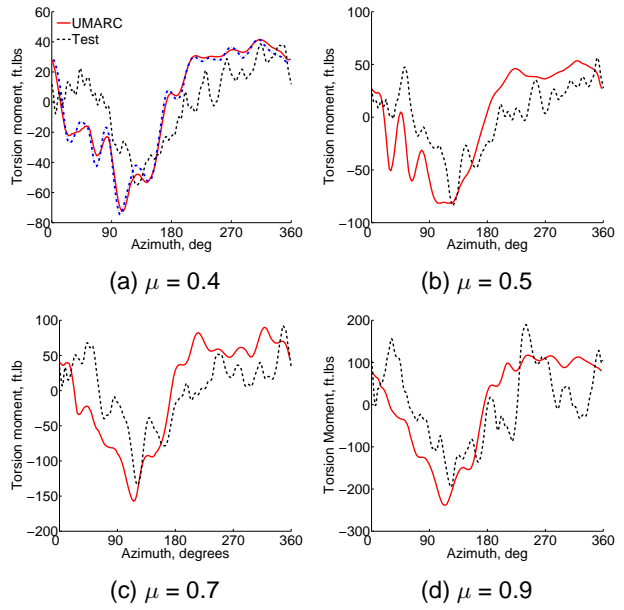


Fig. 16. Oscillatory torsional moment, $r/R = 50\%$. $C_T/\sigma = 0.062$, $\alpha_s = 4^\circ$ aft.

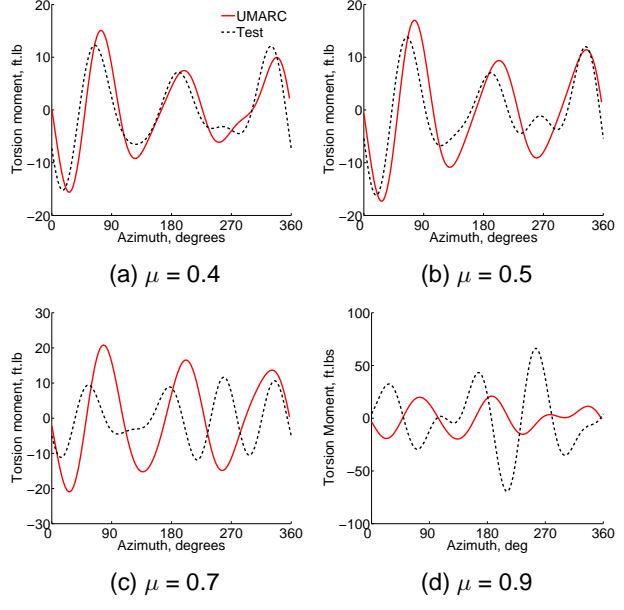


Fig. 17. Vibratory (3-5/rev) torsional moment, $r/R = 50\%$. $C_T/\sigma = 0.062$, $\alpha_s = 4^\circ$ aft.

5. CONCLUSIONS

This paper has evaluated performance and loads predicted by the comprehensive analysis code UMARC for the UH-60A slowed rotor wind tunnel tests. The following conclusions are drawn from this study:

1. The analysis under-predicts thrust by about C_T/σ of 0.012 at zero degrees collective. The sensitivity of thrust to collective is satisfactorily predicted up to $\mu = 0.7$. For higher advance ratios, UMARC predicts a larger positive thrust sensitivity to collective than the test data, which tend towards zero at $\mu = 1.0$.
2. Shaft power is overpredicted by the analysis for all advance ratios. At zero degrees collective, UMARC shows the shaft power increasing with advance ratio, where it is decreasing in the test data. The test shows the shaft power decreasing with collective at advance ratios greater than 0.7 and this trend is captured by the analysis.
3. The rotor drag force is significantly underpredicted if the drag associated with the blade shank is ignored. Modeling the region inboard of the traditional root cut-out ($r/R = 20\%$) with a constant drag coefficient of 0.4 corrects the zero collective drag values but the trends with increasing collectives continue to under-predict the test.
4. The longitudinal pitch cyclic (θ_{1s}) is well predicted until thrust reversal is approached ($\mu < 0.7$) but correlation degrades at higher advance ratios. Lateral pitch cyclic (θ_{1c}) is consistently overpredicted by the analysis by about 2° .
5. The sectional airloads are compared at 92% span for 0° shaft angle and at 22.5% and 92% span for 4° aft shaft tilt. The normal force prediction accurately represents the magnitude and phase of the loading at 92% with a dual wake trailer model when trimming to matched collective. At 22.5% span, it was found that modeling the near-wake up the blade shank (13% span) was important to predict the lift on the advancing side. Lift on the retreating side is overpredicted by UMARC. High frequency loading near 0° azimuth was caused by blade interactions with wake from the inboard blade edge.
6. The sectional pitching moments are poorly predicted. At 22.5% span, the nose up pitching moment on the retreating side is overpredicted. At 92% span, the mean trend of the pitching moment is predicted, but the peak on the advancing side is underpredicted.
7. The oscillatory flap-wise bending moment at 50% station is well predicted by the analysis in phase and magnitude. The peak loading on the advancing side is underpredicted by a small amount. The vibratory (3-5/rev) content is dominated by a 3/rev flapping mode and is generally well predicted.
8. The prediction of the mean oscillatory behavior of the torsional moments at 50% span is fair but the high frequency ($> 12/\text{rev}$) content is missing in the analysis. The vibratory torsional moments are well predicted at $\mu = 0.4$ and 0.5 but breaks down at 0.7.

Acknowledgments

This work is sponsored by the Israel Ministry of Defense, "Aeromechanics of Rotorcraft in High Speed Flight," Grant No. 4440560176 with technical monitor Dr. Avi Weinreb. Many technical discussions with Dr. Omri Rand (Technion) are highly appreciated.

The authors would also like to acknowledge technical assistance from Dr. Anubhav Datta, as well as the support from Dr. Tom Norman of NASA, for providing the UH-60A test data.

References

- ¹Wheatley, J. B. and Hood, M. L., "Full-Scale Wind-Tunnel Tests of a PCA-2 Autogiro Rotor," NACA Report No. 515, 1935
- ²Jenkins, J. L., "Wind-Tunnel Investigation of a Lifting Rotor Operating at Tip-Speed Ratios from 0.65 to 1.45," NASA TN D-628, 1965
- ³McCloud, J. L., Bibbers, J. C., and Stroub, R. H., "An Investigation of Full-Scale Helicopter Rotors at High Advance Ratios and Advance Ratios and Advancing Tip Mach Numbers," NASA TN D-4632, July 1968
- ⁴Charles, B. D., and Tanner, W. H., "Wind Tunnel Investigation of Semirigid Full-Scale Rotors Operating at High Advance Ratios," United States Army Aviation Material Laboratories TR 69-2, January 1969.
- ⁵Yeo, H., Johnson, W., "Optimum Design of a Compound Helicopter," *Journal of Aircraft*, Vol. 46, No. 4, July-August 2009
- ⁶Floros, M., Johnson, W., "Performance analysis of the Slowed-Rotor Compound Helicopter Configuration," *Journal of the American Helicopter Society*, Vol. 54, 2009
- ⁷Ormiston, R., "Rotor Aerodynamic Characteristics at High Advance Ratio Relevant to compound Rotorcraft," American Helicopter Society Future Vertical Lift Aircraft Design Conference, San Francisco, CA, January, 2012.
- ⁸Norman, T. R., Shinoda, P. M., Peterson, R. L., and Datta, A., "Full-scale Wind Tunnel Test of the UH-60A Airloads Rotor," American Helicopter Society 67th Annual Forum, Virginia Beach, VA, May 3-5, 2011.

⁹Datta, A., Yeo, H., and Norman, T. R., "Experimental Investigation and Fundamental Understanding of a Slowed UH-60A Rotor at High Advance Ratios," American Helicopter Society 67th Annual Forum, Virginia Beach, VA, May 3-5, 2011.

¹⁰Kottapalli, S., "Performance and Loads Correlation of a UH-60A Slowed Rotor at High Advance Ratios," American Helicopter Society Future Vertical Lift Aircraft Design Conference, San Francisco, CA, January, 2012.

¹¹Yeo, H., "Investigation of UH-60A Rotor Performance and Loads at High Advance Ratios," *Journal of Aircraft*, Vol. 50, No. 2, March-April 2013, pp 576-589

¹²Johnson, W., "Technology Drivers in the Development of CAMRAD II," American Helicopter Society Aeromechanics Specialists Meeting, San Francisco, CA, January, 1994.

¹³Ormiston, R., "Rotor Aerodynamic Characteristics at High Advance ratios Relevant to Compound Rotorcraft," American Helicopter Society Future Vertical Lift Aircraft Design Conference, San Francisco, CA, January 18-20, 2012.

¹⁴Potsdam, M., Datta, A., and Jayaraman, B., "Computational Investigation and Fundamental Understanding of a Slowed UH-60A Rotor at High Advance Ratios," American Helicopter Society 68th Annual Forum, Fort Worth, TX, May 1-3, 2012.

¹⁵Potsdam, M., Yeo, H., and Ormiston, R., "Performance and Loads Predictions of a Slowed UH-60A Rotor at High Advance Ratios," 39th European Rotorcraft Forum, Moscow, Russia, September 3-6, 2013.

¹⁶Bowen-Davies, G., and Chopra, I., "Investigation of the UH-60A Slowed Rotor Wind Tunnel Tests using UMARC," American Helicopter Society 69th Annual Forum, Phoenix, AZ, May 21-23, 2013.

¹⁷Berry, B., and Chopra, I., "Wind Tunnel Testing for Performance and Vibratory Loads of a Variable-Speed Mach-Scaled Rotor," American Helicopter Society 67th Annual Forum, Virginia Beach, VA, May 3-5, 2011.

¹⁸Berry, B., and Chopra, I., "Performance and Vibratory Load Measurements of a Slowed-Rotor at High Advance Ratios," American Helicopter Society 68th Annual Forum, Fort Worth, TX, May 1-3, 2012.

¹⁹Berry, B., and Chopra, I., "High-Advance Ratio Wind Tunnel Testing of Two Mach Scaled Rotors," American Helicopter Society 69th Annual Forum, Phoenix, AZ, May 21-23, 2013.

²⁰Berry, B., and Chopra, I., "High-Advance Ratio Wind Tunnel Testing of a Model Rotor with Pressure Measurements," American Helicopter Society Aeromechanics Specialists Conference, San Francisco, CA, January 20-24, 2014.

²¹Bowen-Davies, G., and Chopra, I., "Validation of Rotor Performance and Loads at High Advance Ratio," Fifth Decennial AHS Aeromechanics Specialists Conference, San Francisco, CA, January 22-24, 2014.

²²Berry, B., and Chopra, I., "Slowed Rotor Wind Tunnel Testing of an Instrumented Rotor at High Advance Ratio," 40th European Rotorcraft Forum, Southampton, England, September 2-5, 2014.

²³Kufeld, R. M., Balough, D., Cross, J. L., Studebaker, K. F., Jennison, C. D., and Bousman, W. G., "Flight Testing the UH-60A Airloads Aircraft," American Helicopter Society 50th Annual

²⁴Chopra, I. and Bir, G., "University of Maryland Advanced Code: UMARC," American Helicopter Society Aeromechanics Specialists Conference, San Francisco, CA, January 1994.

²⁵Bagai, A., Leishman, J.G., "Rotor Free-Wake Modeling using a Relaxation Technique - Including Comparisons with Experimental Data," *Journal of the American Helicopter Society*, Vol. 40, (2), April 1995

²⁶Leishman, J. G., Beddoes, T. S., "A Semi-Empirical Model for Dynamic Stall," American Helicopter Society 42nd Annual Forum Proceedings, Washington D.C., June 1986.

²⁷Amiriaux, M., Thomas, S., Baeder, J., "Fuselage Modelization for Multi-Fidelity Coupled CFD/CSD Simulation of Rotorcrafts in BVI Condition," 31st AIAA Applied Aerodynamics Conference, San Diego, CA, USA, June 27, 2013

COPYRIGHT STATEMENT

The author(s) confirm that they, and/or their company or organization, hold copyright on all of the original material included in this paper. The authors also confirm that they have obtained permission, from the copyright holder of any third party material included in this paper, to publish it as part of their paper. The author(s) confirm that they give permission, or have obtained permission from the copyright holder of this paper, for the publication and distribution of this paper as part of the ERF2014 proceedings or as individual offprints from the proceedings and for inclusion in a freely accessible web-based repository.